

# Supporting Information

A Solvent-Free One-pot Multicomponent Tandem  
Polymerization of 3,4-Dihydropyrimidin-2(1*H*)-ones  
(DHPMs) Catalyzed by Ionic-Liquid@Fe<sub>3</sub>O<sub>4</sub> NPs:  
Development of Polyamide Gels

Manpreet Kaur,<sup>a</sup> Mayank,<sup>b</sup> Deepak Bains,<sup>b</sup> Gagandeep Singh,<sup>b</sup> Navneet Kaur<sup>\*a</sup> and Narinder  
Singh<sup>\*b</sup>

<sup>a</sup>Department of Chemistry, Panjab University, Chandigarh, India, 160014, E-mail:  
[navneetkaur@pu.ac.in](mailto:navneetkaur@pu.ac.in); Tel: +91-0172-2534405

<sup>b</sup>Department of Chemistry, Indian Institute of Technology Ropar (IIT Ropar), Rupnagar, Punjab,  
140001, India. E-mail: [nsingh@iitrpr.ac.in](mailto:nsingh@iitrpr.ac.in); Tel: +91-1881242176

## Contents

**Procedure S1.** Synthesis of IL1.

**Procedure S2.** Preparation of Iron Oxide Nanoparticles.

**Table S1:** Yield percentage, molecular weight and solubility of synthesized MCTPs P1-P8.

**Figure S1:** GPC traces of synthesized polyamides P1-P8.

**Figure S2:** Mass spectra of Biginelli Product (B1).

**Figure S3: A)** FT-IR spectra of B1 with N-H and C=O stretching vibrations at  $3336.8\text{ cm}^{-1}$  and  $1694.6\text{ cm}^{-1}$  whereas in P1, shifted at  $3473\text{ cm}^{-1}$  and  $1602.6\text{ cm}^{-1}$  respectively. **B)** Comparison of  $^1\text{H}$  NMR spectra of B1 and P1 in  $\text{CDCl}_3/\text{DMSO-}d_6$ .

**Figure S4:** FT-IR spectra of polyamide adducts P2-P8.

**Figure S5: A)**  $^1\text{H}$  NMR Spectra in mixture of  $\text{CDCl}_3$  and  $\text{DMSO-}d_6$  of P1-P4 (Urea derivatives). **B)**  $^1\text{H}$  NMR Spectra in mixture of  $\text{CDCl}_3$  and  $\text{DMSO-}d_6$  of P5-P8 (thiourea derivatives).

**Figure S6: A)**  $^{13}\text{C}$  NMR Spectra in mixture of  $\text{CDCl}_3$  and  $\text{DMSO-}d_6$  of P1-P4 (Urea derivatives). **B)**  $^{13}\text{C}$  NMR Spectra in mixture of  $\text{CDCl}_3$  and  $\text{DMSO-}d_6$  of P5-P8 (thiourea derivatives).

**Figure S7:** Photos of synthesized Polyamide gels (P1-P8).

**Figure S8:** (A) Mass spectrum of IL1 and (B) Mass spectrum of IL-2.

**Figure S9:** (A) FT-IR spectrum of IL1 and (B) FT-IR spectrum of IL-2.

**Figure S10: (A-C)** SEM, TEM and HR-TEM images of  $\text{IL2@Fe}_3\text{O}_4$  NPs respectively. (D-F) SEM, TEM and HR-TEM images of  $\text{IL1@Fe}_3\text{O}_4$  NPs respectively.

**Figure S11: (A-B)** DLS of  $\text{IL1-2@Fe}_3\text{O}_4$ ; **(C-D)** EDX of  $\text{IL1-2@Fe}_3\text{O}_4$ .

**Figure S12:** Solid state UV-Vis absorption spectra of  $\text{Fe}_3\text{O}_4$  NPs, IL1-2 and  $\text{IL1-2@Fe}_3\text{O}_4$ ; **C)** Solid state emission profile IL1 and  $\text{IL1@Fe}_3\text{O}_4$  NPs, IL2 and  $\text{IL1@Fe}_3\text{O}_4$  NPs.

**Figure S13:** A) TGA-Plot of  $\text{Fe}_3\text{O}_4$ ,  $\text{IL1@Fe}_3\text{O}_4$  and  $\text{IL2@Fe}_3\text{O}_4$ . B)  $\text{N}_2$  adsorption isotherm of  $\text{Fe}_3\text{O}_4$ ,  $\text{IL-1@Fe}_3\text{O}_4$  and  $\text{IL-2@Fe}_3\text{O}_4$

**Table S2:**  $\text{N}_2$  adsorption BET measurements of  $\text{Fe}_3\text{O}_4$ ,  $\text{IL-1@Fe}_3\text{O}_4$  and  $\text{IL-2@Fe}_3\text{O}_4$

**Table S3:** Acidic strength calculation for  $\text{Fe}_3\text{O}_4$ ,  $\text{IL-1@Fe}_3\text{O}_4$  and  $\text{IL-2@Fe}_3\text{O}_4$

**Figure S14: A-B)** SEM and DLS images of  $\text{IL2@Fe}_3\text{O}_4$  after the fifth recycling cycle, respectively; **C-D)** SEM and DLS images of  $\text{IL2@Fe}_3\text{O}_4$  after the tenth recycling cycle, respectively.

**Table S4:** Physical Properties and Efficiency of Recovered  $\text{IL2@Fe}_3\text{O}_4$  NPs catalyst.

**Procedure S1. Synthesis of IL1:** IL1 was synthesized by using reported procedure.<sup>1</sup> Dissolved 1 eq of 1-methyl imidazole in acetonitrile solvent and then added 1eq of bromoacetic acid and refluxed the reaction mixture at  $80^\circ\text{C}$  for 6 hours. Pale yellow colored crystalline solid was separated after evaporation of the solvent on reduced pressure. Yield 74% and purity was characterized by IR (KBr thin film),  $\nu(\text{cm}^{-1})$ : 3378.66 (broad), 3092.63, 3040.17, 1719.50, 1666.89, 1565.97, 1366.71, 1174.45, 1044.71, 771.36, 648.85, 455.78. ESI-MS  $m/z = 141.07$  [ $\text{M} + \text{H}$ ]<sup>+</sup>.

**Procedure S2. Preparation of Iron Oxide Nanoparticles:** The iron oxide nanoparticles were prepared by using reported procedure.<sup>2</sup> Dissolved  $\text{FeSO}_4 \cdot 7\text{H}_2\text{O}$  in 100 ml of double distilled water to form a 0.1 M solution and dropwise added 0.45 M solution of NaOH as precipitating agent with continuous stirring. The black precipitates separated out after 45 min stirring. Filtered the precipitates and washed with water/ethanol mixture for 3 to 4 times.

**Table S1:** MCTPs of poly(DHPMs) (P1-P8).

Entry	Poly(DHPMs)	Yield (%)	$M_w^a$ (g/mol)	PDI <sup>a</sup>	Solubility <sup>b</sup>
1.	P1	75	41,712	1.67	✓
2.	P2	70	37,315	1.20	✓
3.	P3	74	18,525	1.36	✓
4.	P4	80	83,384	1.78	✓

5.	P5	74	17,332	1.52	✓
6.	P6	70	11,427	1.75	✓
7.	P7	68	13,375	1.27	✓
8.	P8	75	35,860	1.65	✓

<sup>a</sup>Evaluated by GPC at room temperature in THF solvent and calibrated by linear polystyrene.

<sup>b</sup>Solubility tested in organic solvents, such as Metanol, THF, DMSO, DMF and Acetonitrile:

✓ = Completely soluble.

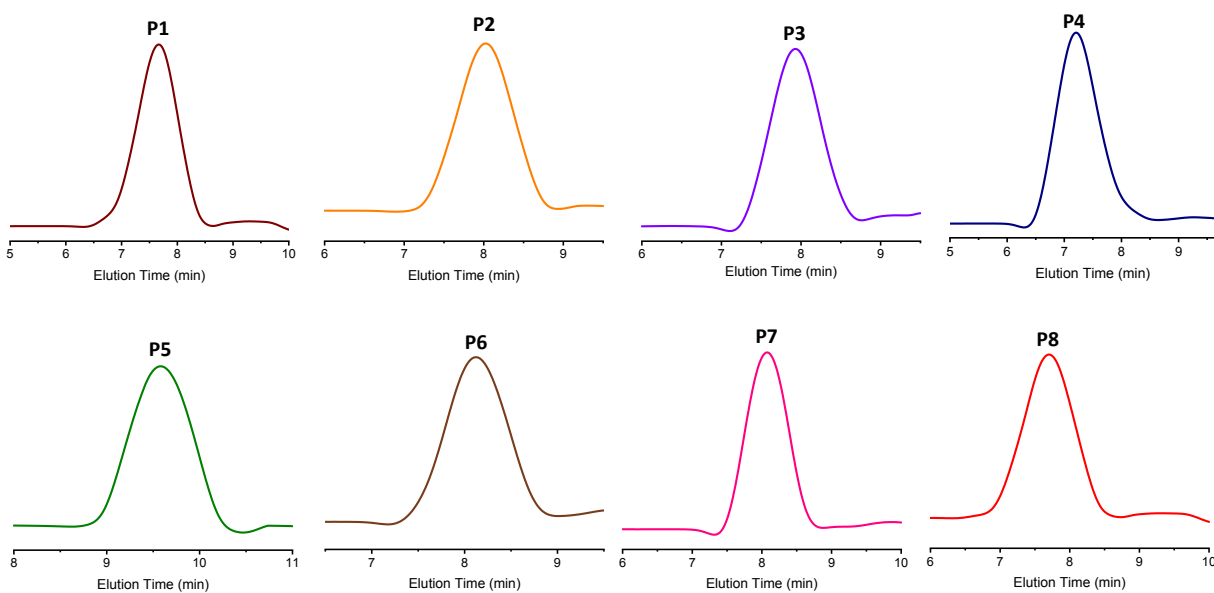


**Figure S1.** GPC traces of synthesized polyamides P1-P8.

Monoisotopic Mass, Odd and Even Electron Ions  
 25 formula(e) evaluated with 1 results within limits (up to 50 best isotopic matches for each mass)

Elements Used:

C: 10-25 H: 10-30 N: 0-4 O: 0-6

Sample Name : MR-19

INDIAN INSTITUTE OF TECHNOLOGY

XEVO G2-XS QTOF

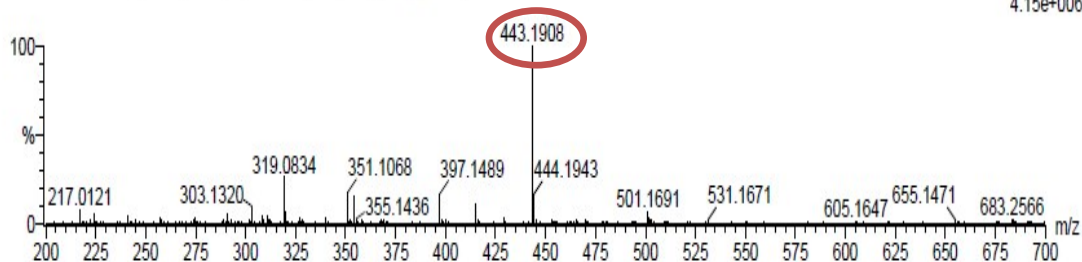
Test Name : HRMS

ROPAR

170717-MR-19 19 (0.214) AM2 (Ar,18000.0,0.00,0.00); Cm (19:28)

1: TOF MS ES+

4.15e+006



Minimum: -1.5  
 Maximum: 5.0 20.0 50.0

Mass	Calc. Mass	mDa	PPM	DBE	i-FIT	Norm	Conf(%)	Formula
443.1908	443.1931	-2.3	-5.2	11.5	448.2	n/a	n/a	C22 H27 N4 O6

**Figure S2.** Mass spectra of Biginelli Product (B1).

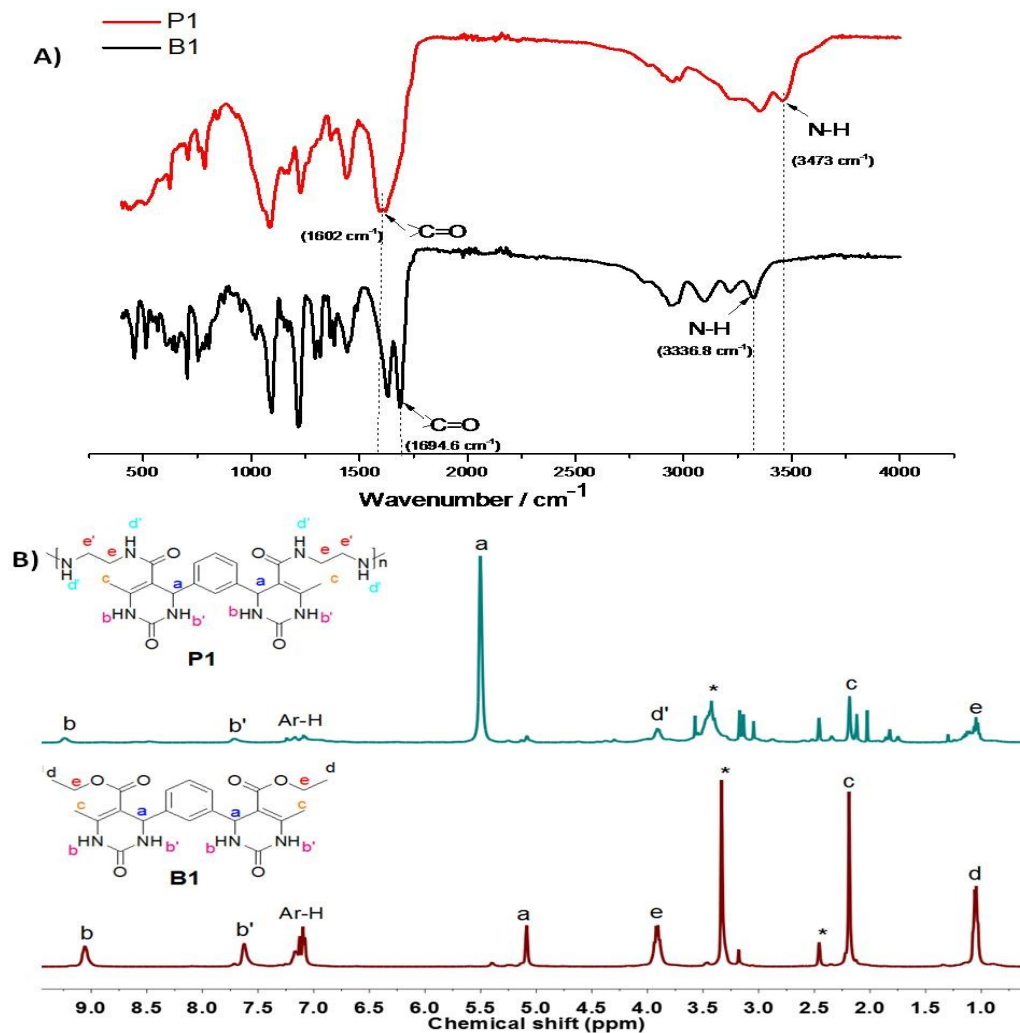


**Figure S3:** **A)** FT-IR spectra of B1 with N-H and C=O stretching vibrations at  $3336.8 \text{ cm}^{-1}$  and  $1694.6 \text{ cm}^{-1}$  whereas in P1, shifted at  $3473 \text{ cm}^{-1}$  and  $1602.6 \text{ cm}^{-1}$  respectively. **B)** Comparison of  $^1\text{H}$  NMR spectra of B1 and P1 in  $\text{CDCl}_3/\text{DMSO-}d_6$ .

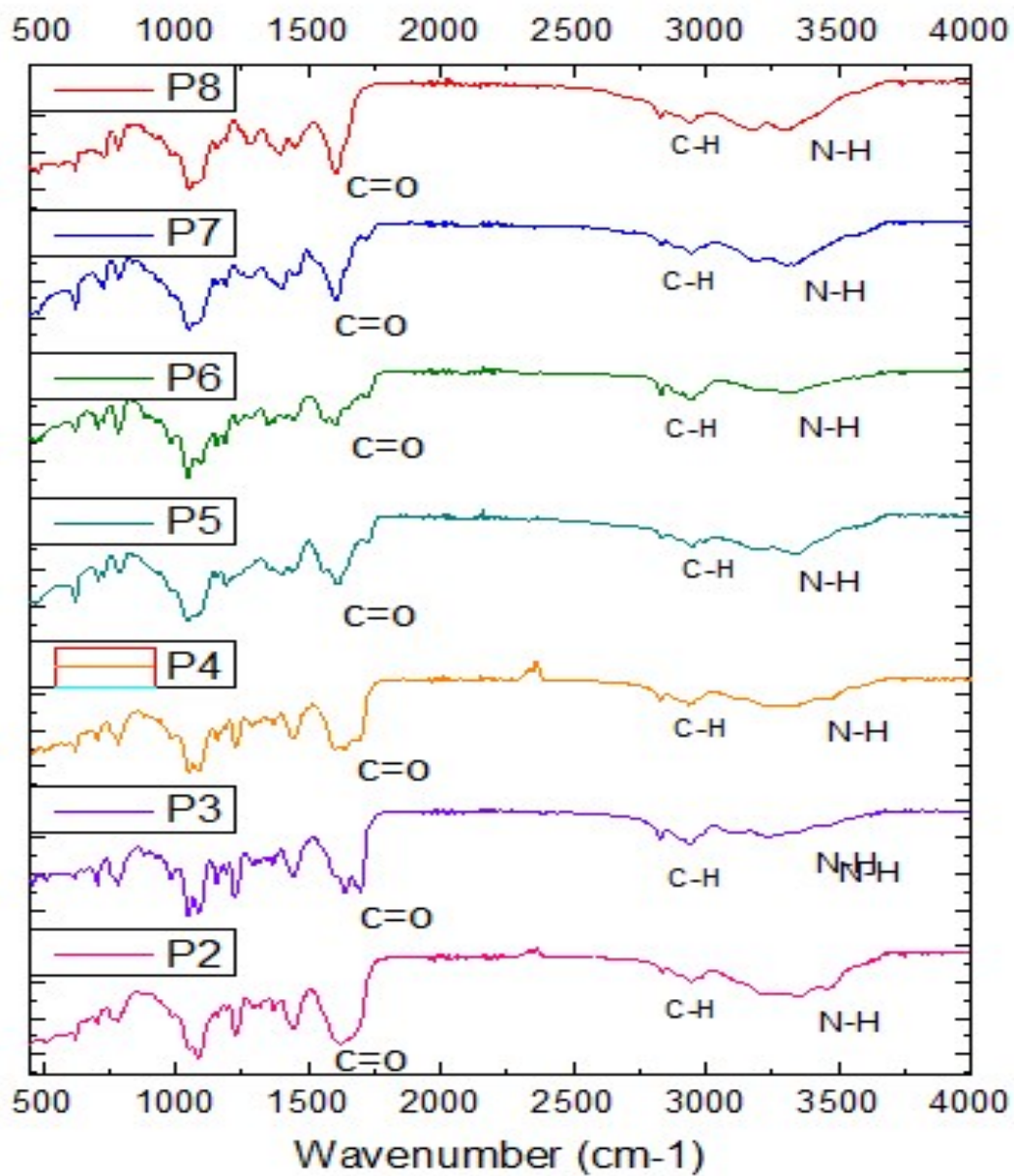


**Figure S4.** FT-IR spectra of polyamide adducts P2-P8.

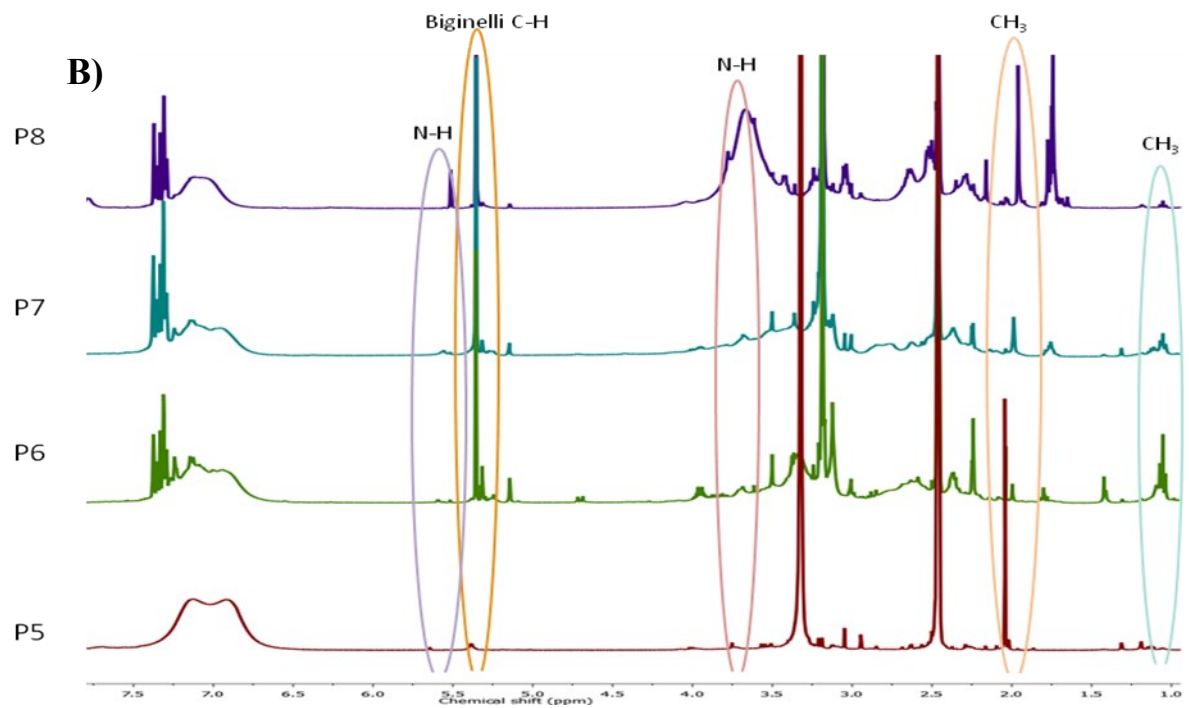
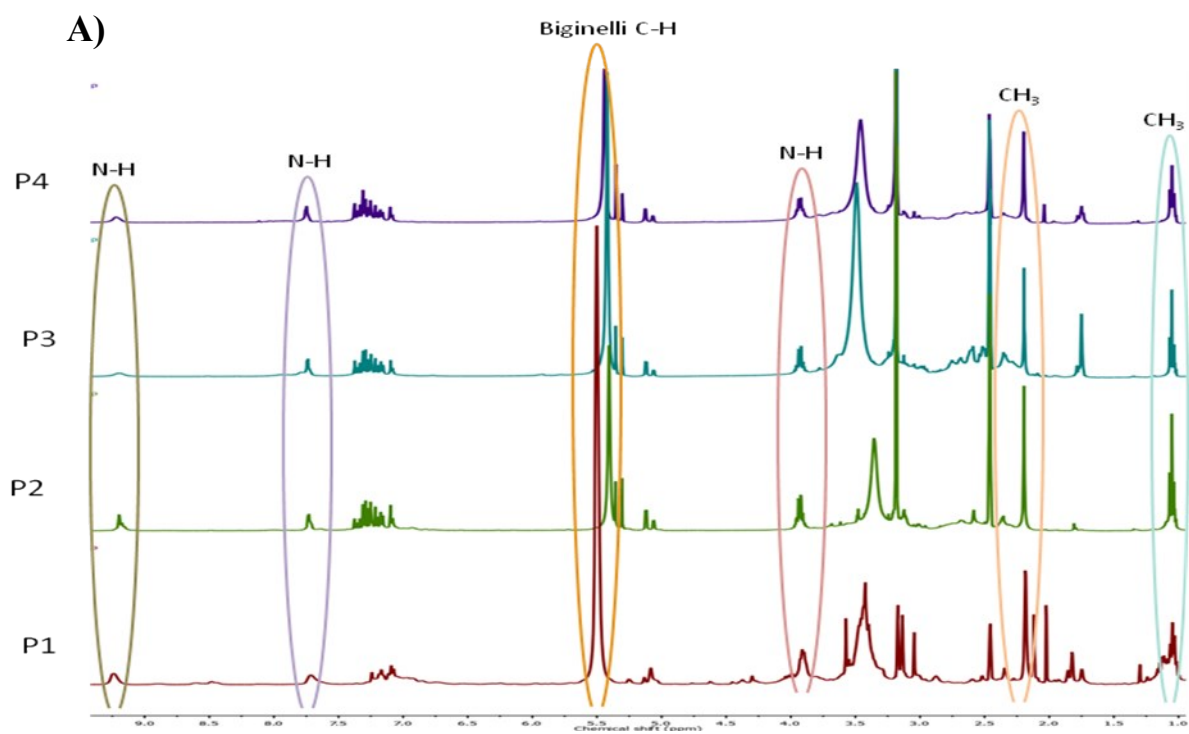


**Figure S5.:** A)  $^1\text{H}$  NMR spectra in mixture of  $\text{CDCl}_3$  and  $\text{DMSO-}d_6$  of P1-P4 (Urea derivatives). B)  $^1\text{H}$  NMR spectra in mixture of  $\text{CDCl}_3$  and  $\text{DMSO-}d_6$  of P5-P8 (thiourea derivatives).



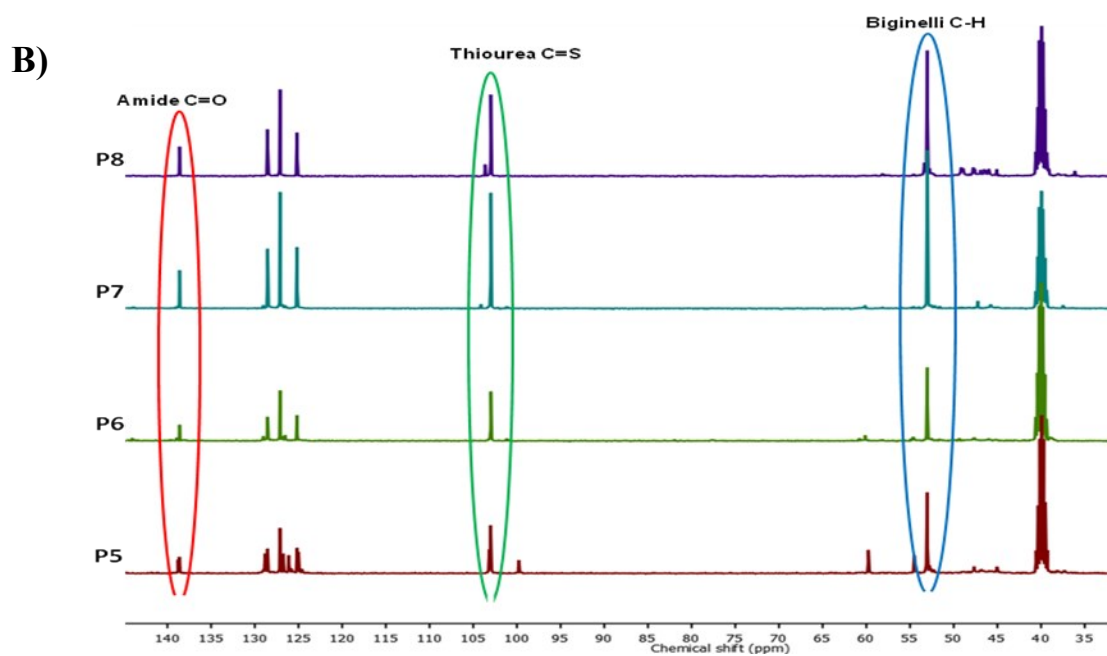
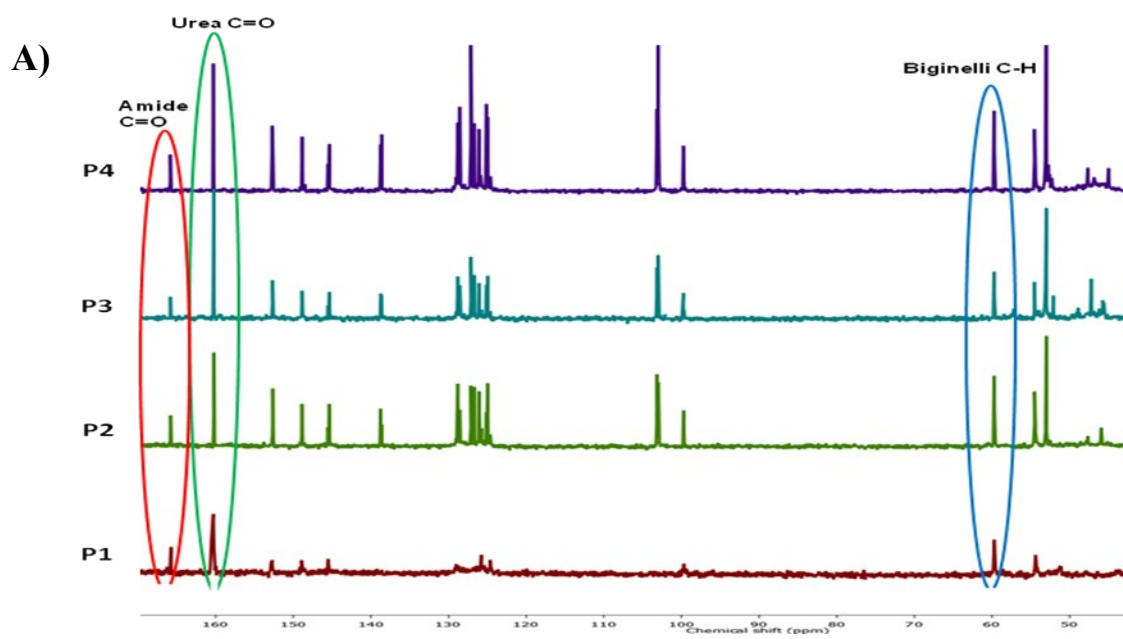


**Figure S6. A)**  $^{13}\text{C}$  NMR spectra in mixture of  $\text{CDCl}_3$  and  $\text{DMSO-}d_6$  of P1-P4 (Urea derivatives). **B)**  $^{13}\text{C}$ -NMR spectra in mixture of  $\text{CDCl}_3$  and  $\text{DMSO-}d_6$  of P5-P8 (thiourea derivatives).

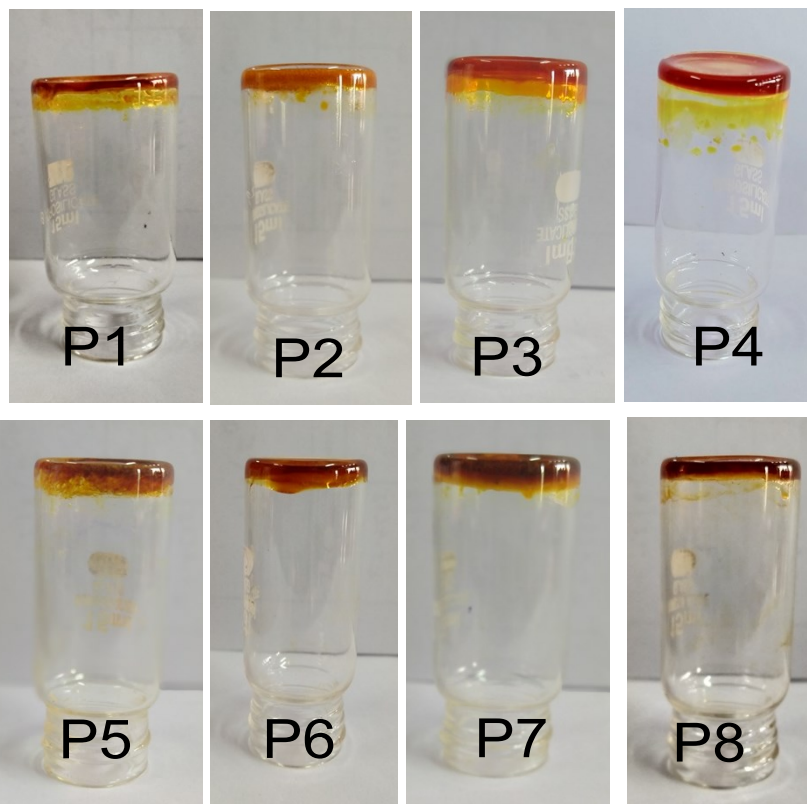
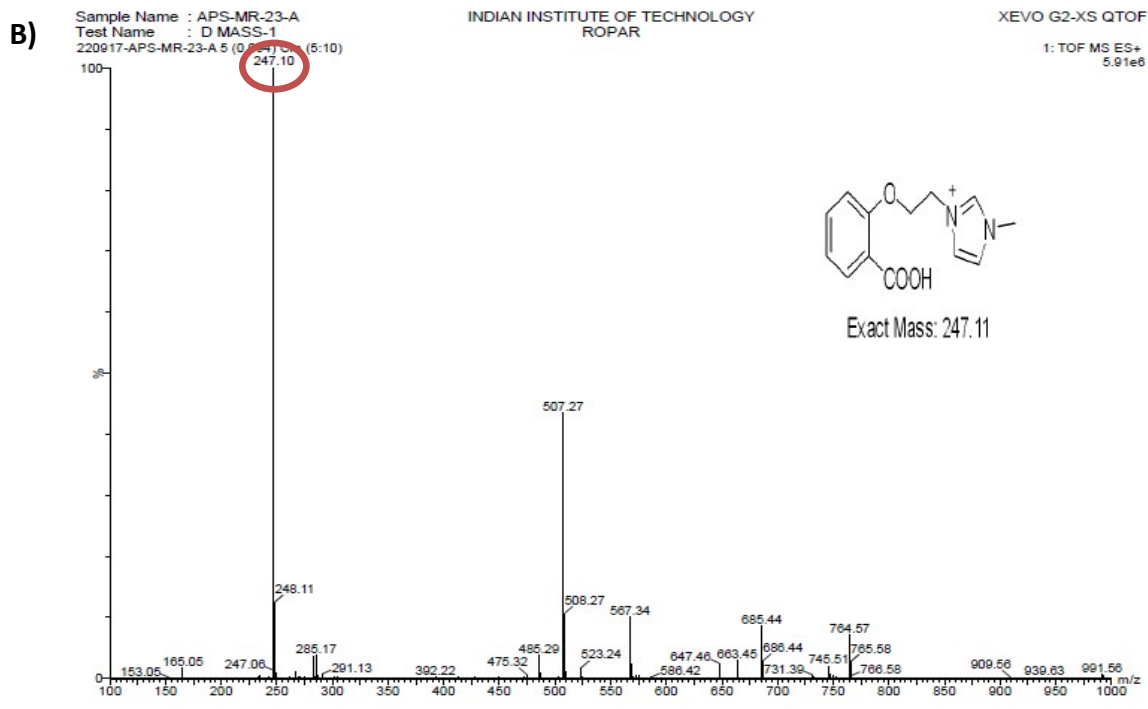
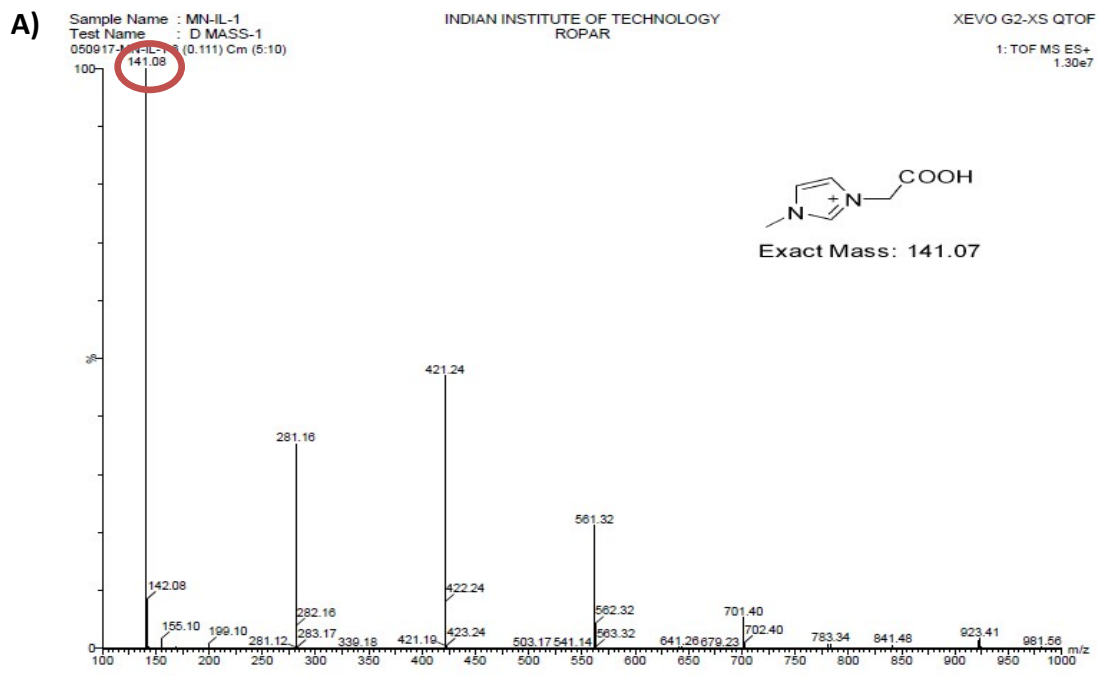
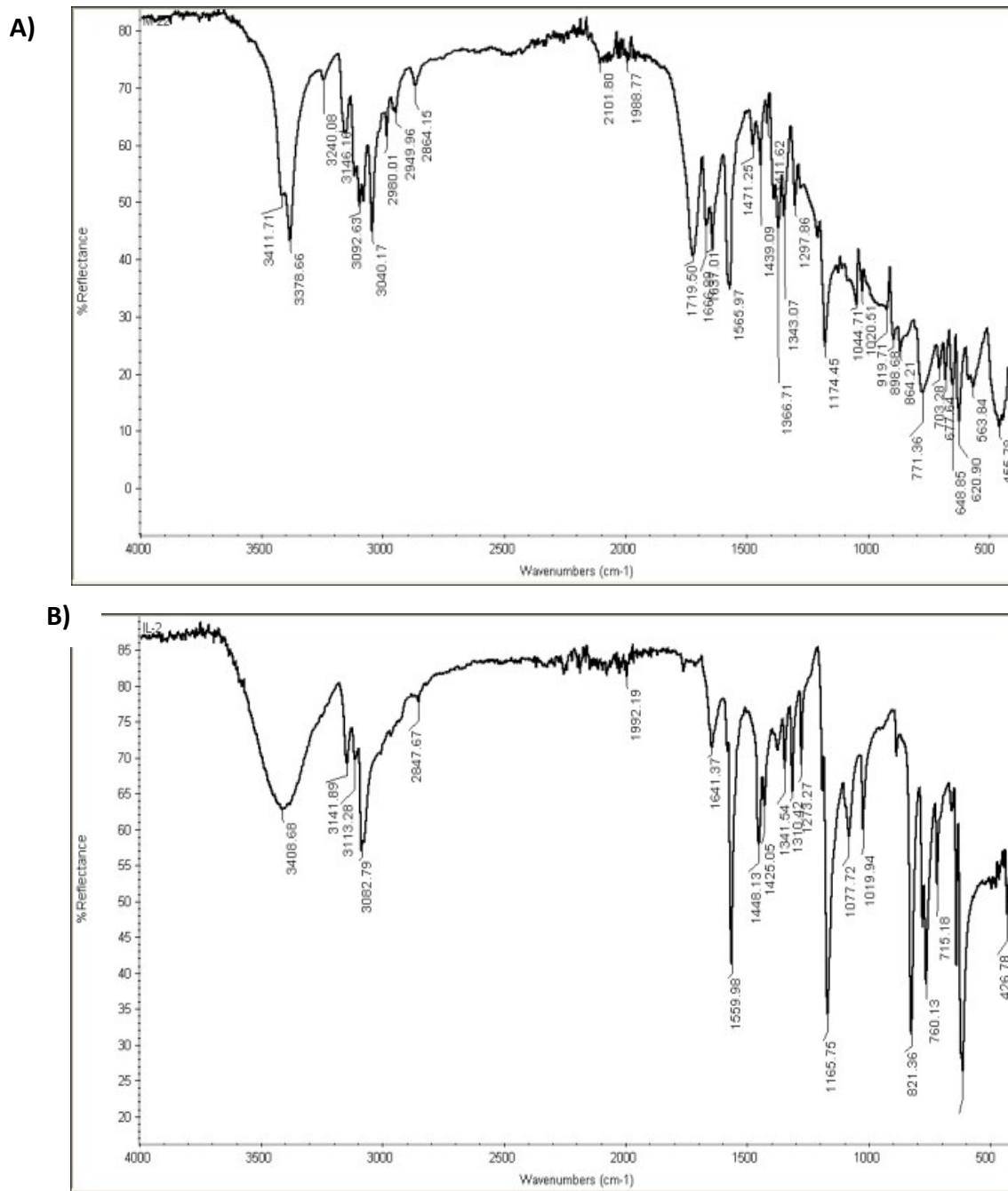


Figure S7: Photographs of Synthesized polyamide gels (P1-P8).



**Figure S8.** (A) Mass spectrum of IL1 and (B) Mass spectrum of IL-2.



**Figure S9.** (A) FT-IR spectrum of IL1 and (B) FT-IR spectrum of IL-2.

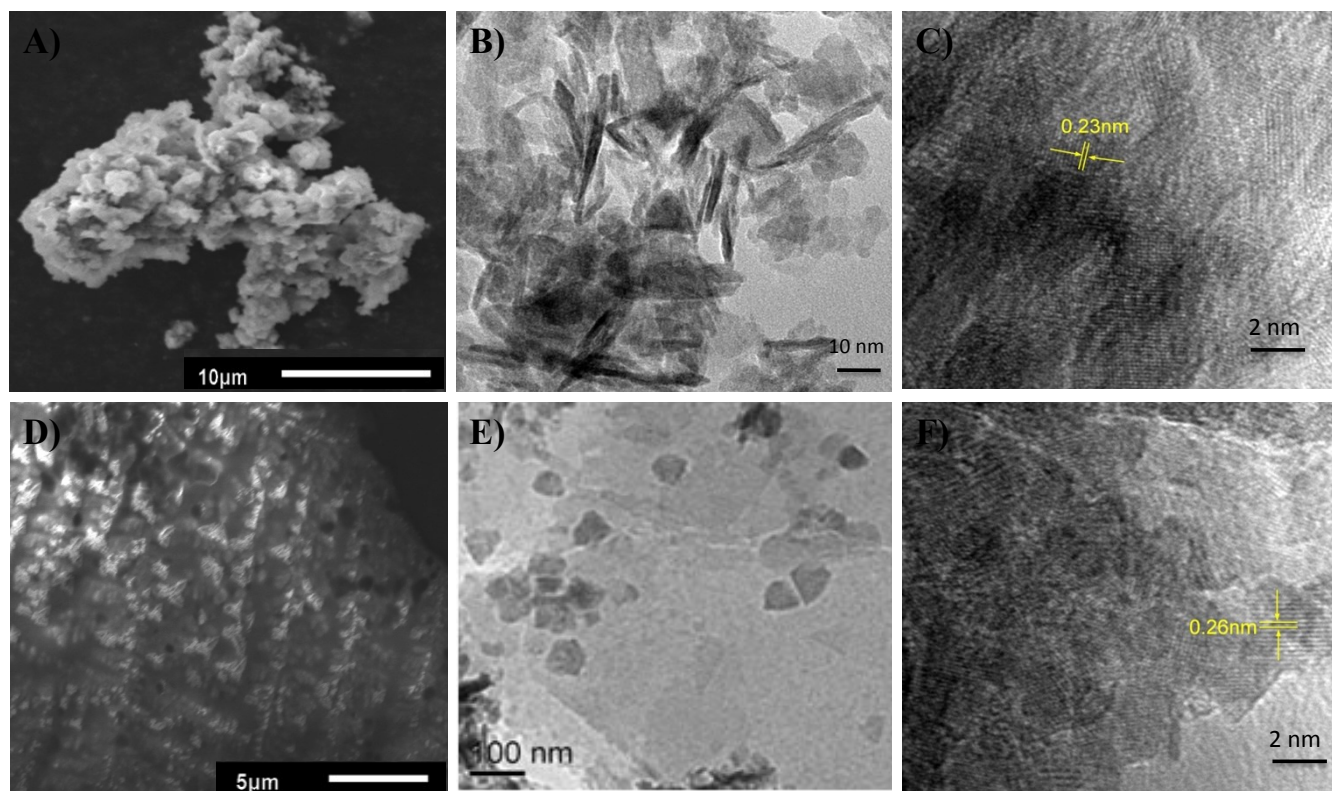


**Figure S10:** (A-C) SEM, TEM and HR-TEM images of IL2@Fe<sub>3</sub>O<sub>4</sub> NPs respectively. (D-F) SEM, TEM and HR-TEM images of IL1@ Fe<sub>3</sub>O<sub>4</sub> NPs respectively.

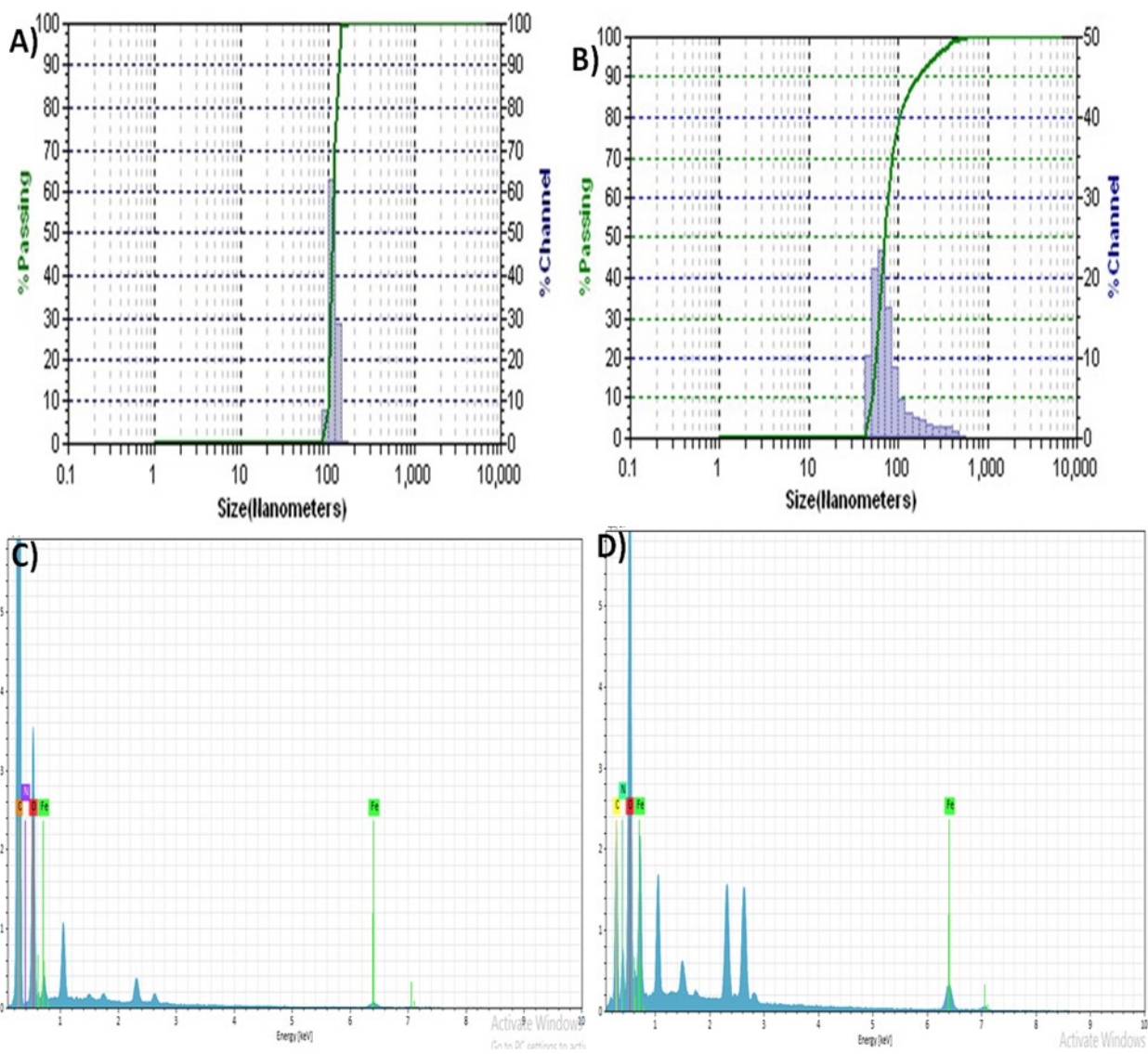


**Figure S11. A-B) DLS of IL1-2@Fe<sub>3</sub>O<sub>4</sub>; C-D) EDX of IL1-2@Fe<sub>3</sub>O<sub>4</sub>.**



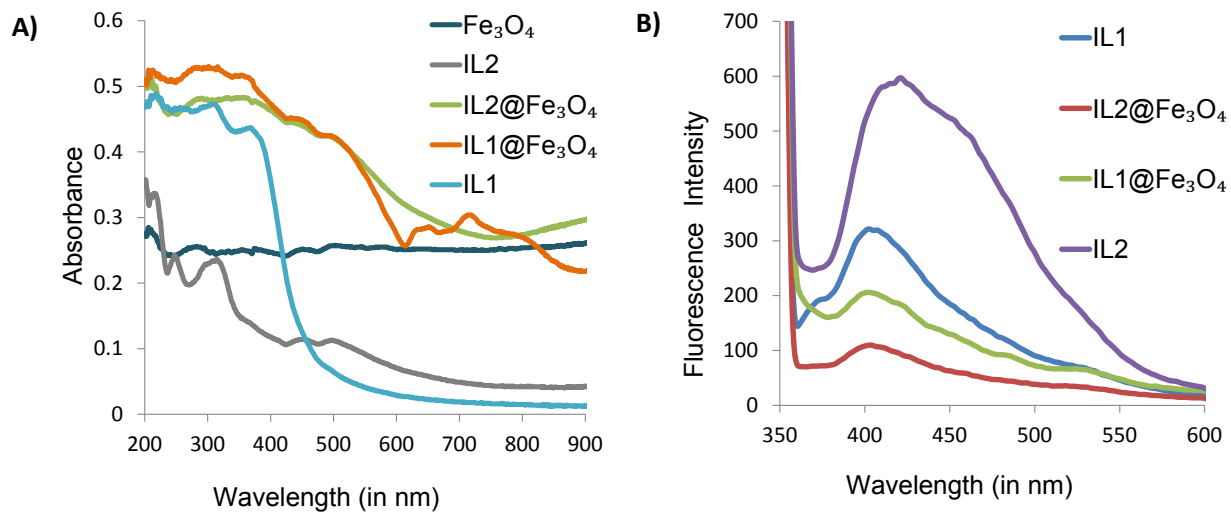


**Figure S12:** A) Solid state UV-Vis absorption spectra of Fe<sub>3</sub>O<sub>4</sub> NPs, IL1-2 and IL1-2@Fe<sub>3</sub>O<sub>4</sub>; B) Solid state emission profile IL1 and IL1@Fe<sub>3</sub>O<sub>4</sub>NPs, IL2 and IL1@Fe<sub>3</sub>O<sub>4</sub>NPs.

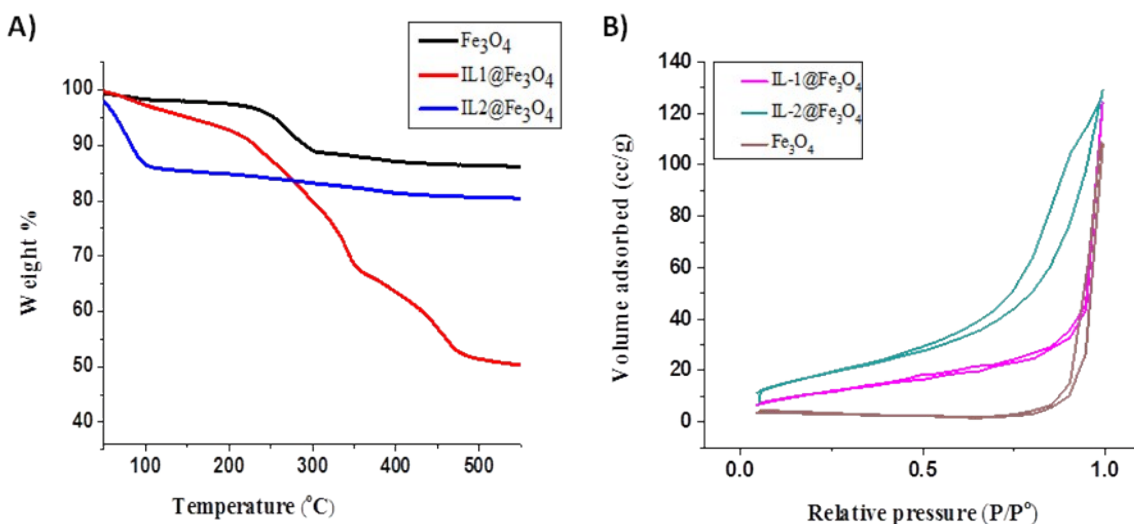


**Figure S13.** A) TGA-Plot of Fe<sub>3</sub>O<sub>4</sub>, IL1@Fe<sub>3</sub>O<sub>4</sub> and IL2@Fe<sub>3</sub>O<sub>4</sub>. B) N<sub>2</sub> adsorption isotherm of Fe<sub>3</sub>O<sub>4</sub>, IL-1@Fe<sub>3</sub>O<sub>4</sub> and IL-2@Fe<sub>3</sub>O<sub>4</sub>.

**Table S2:** N<sub>2</sub> adsorption BET measurements of Fe<sub>3</sub>O<sub>4</sub>, IL-1@Fe<sub>3</sub>O<sub>4</sub> and IL-2@Fe<sub>3</sub>O<sub>4</sub>

S. No.	Catalyst	Surface area (m <sup>2</sup> g <sup>-1</sup> )	Pore volume (cm <sup>3</sup> g <sup>-1</sup> )	Average pore diameter (nm)
1.	Fe <sub>3</sub> O <sub>4</sub>	18.00	0.181	32.55
2.	IL-1@Fe <sub>3</sub> O <sub>4</sub>	57.57	0.198	3.77
3.	IL-2@Fe <sub>3</sub> O <sub>4</sub>	90.63	0.209	9.54

**Table S3:** Acidic strength calculation for Fe<sub>3</sub>O<sub>4</sub>, IL-1@Fe<sub>3</sub>O<sub>4</sub> and IL-2@Fe<sub>3</sub>O<sub>4</sub>

Sr.No	Catalyst	Volume of 0.5 N HCl <sup>a</sup> (ml)	Basic unit count <sup>b</sup> (BU) (mmol/g)	(RBA) <sup>c</sup> (mmol/g)	Relative basic units <sup>d</sup> (RBA/0.25)
1.	Fe <sub>3</sub> O <sub>4</sub>	0.5	0.25	0.25	1
2.	IL1@Fe <sub>3</sub> O <sub>4</sub>	0.4	0.2	0.63	2.55
3.	IL2@Fe <sub>3</sub> O <sub>4</sub>	0.7	0.35	1.76	7.04

<sup>a</sup>Volume of 0.5 N HCl required to neutralize 1 mg of catalyst (ml) calculated via back titration; <sup>b</sup>Number of unit's equivalent to "OH" present in 1 mg of sample; <sup>c</sup>Relative SA based exposure of BU to reactants, calculated using the formula: BU × SA of catalyst/SA of Fe<sub>3</sub>O<sub>4</sub> (SAs from Table 3); <sup>d</sup>Calculated using the formula: RBA×RBU/RBU for Fe<sub>3</sub>O<sub>4</sub>.



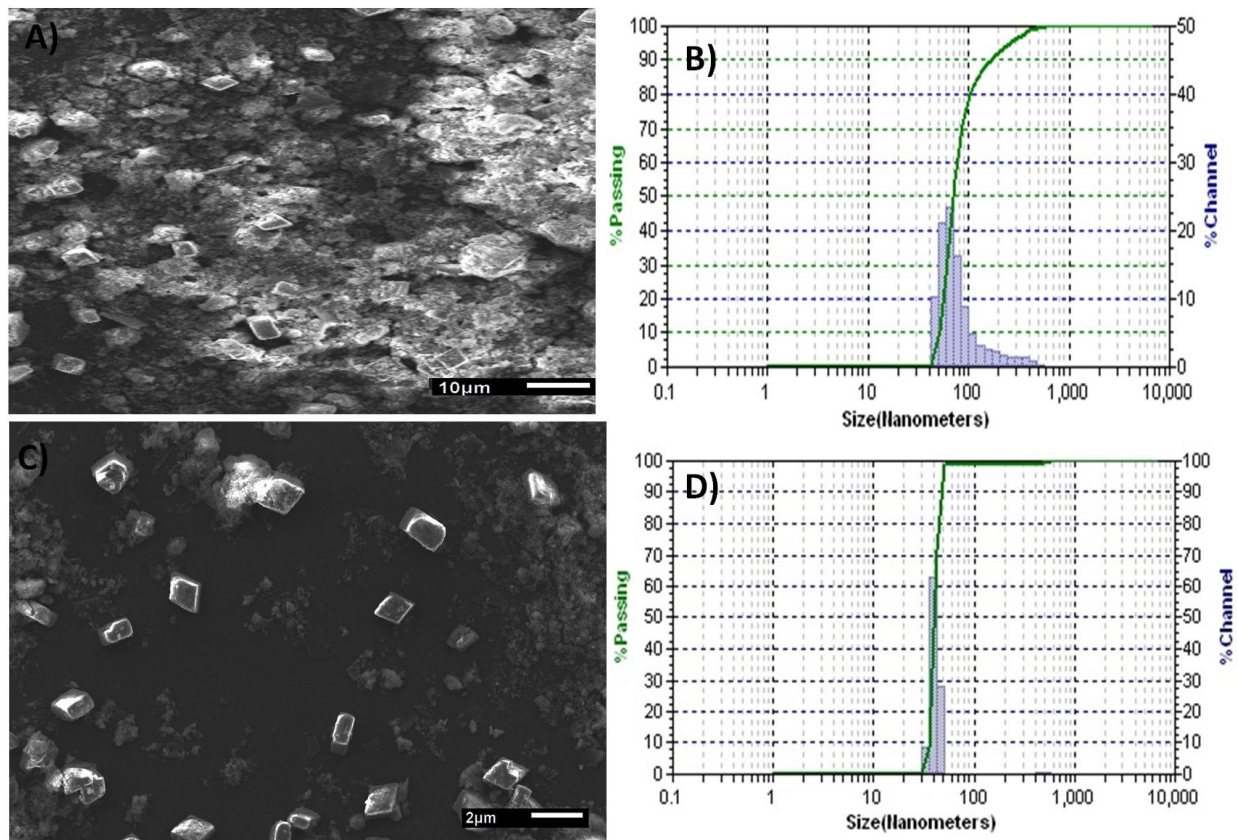


**Figure S14:** A-B) SEM and DLS images of IL2@ Fe<sub>3</sub>O<sub>4</sub> after the fifth recycling cycle, respectively; C-D) SEM and DLS images of IL2@ Fe<sub>3</sub>O<sub>4</sub> after the tenth recycling cycle, respectively.

**Table S4:** Physical Properties and Efficiency of Recovered IL2@Fe<sub>3</sub>O<sub>4</sub> NPs catalyst.

Entry	Catalyst	Size (nm) <sup>a</sup>	(%) Yield of P1
1.	IL2@Fe <sub>3</sub> O <sub>4</sub> <sup>b</sup>	67	91
2.	IL2@Fe <sub>3</sub> O <sub>4</sub> <sup>c</sup>	49	84

<sup>a</sup>Measured by DLS. IL2@Fe<sub>3</sub>O<sub>4</sub> recovered after <sup>b</sup>fifth and <sup>c</sup>tenth catalytic reaction cycle.

## REFERENCES

1. Mayank, A. Singh, P. Raj, R. Kaur, A. Singh, N. Kaur and N. Singh, *New J. Chem.*, **2017**, 41, 3872-3881.
2. D. D. Suppiah and S. B. A. Hamid, *J. Magn. Magn. Mater.*, **2016**, 414, 204-208.